TPS-SURF-SAC Based Matching of Feature Points in Nonrigid Deformed Tissues: Applied to Abdomen MR Images

Xubing Zhang, Shinichi Hirai
Department of Robotics, Faculty of Science and Engineering, Ritsumeikan University, Kusatsu, Shiga 525-8577, Japan.

***Abstract*-Due to the nonlinear deformation of the nonrigid and nonuniform biological tissues, it is difficult whereas important to correctly match a number of feature points distributed somewhat uniform in the tissues from MR images for deformation measurement. In this paper, the authors present TPS-SURF-SAC matching method and mismatching elimination method based on TPS clustering. Firstly the matching region is identified by a TPS for every query point. Then the SURF descriptors and the proposed Spatial Association Correspondence (SAC) method are combined to match the feature points. Finally, using clustering the coordinate differences between the matching points obtained using TPS-SURF-SAC method and the matching points matched by TPS model, most of wrong match points are eliminated. After every iterative processing of matching and mismatching elimination, the updated TPS model becomes more accurate and more correctly matched points can be identified than that of the previous iteration. The experimental results showed that the proposed method outperformed the single SURF and SIFT methods.**

I. INTRODUCTION

ATCHING of feature points is a key component in many computer vision tasks, such as, stereo matching, image guided surgery, motion tracking, pattern identification, and object recognition. In this paper, the application of extraction and matching of feature points is focused on the deformation measurement of nonrigid and nonuniform biological tissues. The deformations of the biological tissues are caused by the forces applied to biological tissues, with the initial and deformed MR images being taken. Deformation measurement aims to obtain the displacements of a number of feature points, which are usually distributed in the inner parts, boundaries and separatrixes of layers in the tissues. In the application and research of biomedical engineering, and surgical simulation using deformation models, the physical characteristics, such as Young's modulus, Poisson's ratio and some unknown parameters have to be available. Measurement of the deformation field of the real nonrigid tissues is the prerequisite for the evaluation of the physical characteristics nonlinearly distributing in the tissues [1]–[5]. Usually the deformations of the biological tissues are irregular. For example, the human body consists of various tissues, such as skin, muscle, organ, bone, and nail, of which the physical parameters are very different resulting in the different deformations with the same force on different tissues. Due to the nonlinear deformation of the nonrigid and nonuniform tissues, it is by no means a trivial task to measure the accurate displacements of a number of feature points distributing on the inner parts, boundaries and separatrixes of layers all over the tissues.

Deformation measurement of nonrigid tissues is not identical with nonlinear registration which aims to find a transformation such that the transformed template is similar to the reference image. Usually, one cannot obtain the accurate displacements of many feature points by the intensity based registration techniques such as FFD (Free Form Deformation) B-Spline and Demons based registration methods [6]–[14]. In feature point based registration methods, the matching of feature points is critical while difficult to be solved in nonlinearly deformed images [15]–[19]. In the famous feature-based nonlinear registration method HAMMER, the attribute vector consisting of GMI (geometric moment invariants) feature, edge type and intensity of the voxel is utilized to identify the driving boundary voxel of registration in the segmented MR images of brain [15]. Nevertheless, the attribute vector of HAMMER cannot be utilized in gray MR images directly, and it is lack of the texture feature of the voxel which is critical for identification of the feature points in other biological tissues such as muscles, fat and visceral organs. Actually, the anatomical correspondences and image similarity are the focuses of nonlinear registration, with smoothness constraint usually being utilized to regularize the transformation of the displacement field. However, to obtain the physical characteristics in the nonrigid and nonuniform tissues, deformation field measurement aims to accurately evaluate the displacements of a number of feature points being somewhat uniformly distributed in the boundaries, separatrixes of layers, and inner parts of the tissues. So that, the nonlinear registration methods would not behave well in deformation measurement for identification of the physical characteristic.

A wide variety of feature point descriptors have already been proposed in the literature [20]–[26]. Shown in the literature [22], the Scale Invariant Feature Transform SIFT [20] outperforms the other feature descriptors like Gaussian derivatives [23], moment invariants [24], phase-based local features. Various refinements on the SIFT scheme have been proposed, the PCA-SIFT and the GLOH methods are known well in them [21], [22]. Bay presented SURF (Speeded-UP

Robust Feature) [25], which is more repeatable, distinctive, and robust than SIFT. He also proved that, SURF outperformed the other methods such as GLOH and PCA-SIFT [22], [25], [26]. However, SIFT and SURF is not invariant to general deformations [21], [27]. Actually, when we attempted to evaluate the deformation measurement by SURF and SIFT, the experimental results were not inspiring.

Ling and Jacobs proposed a deformation descriptor called GIH based on geodesic distance [27]. One drawback is that it assumes the deformation along different directions to be isotropic. This assumption is usually not true in practice [28]. Tian proposed a low-complexity deformation by using Hilbert scanning [29]. But if an interest point is located in the subdivision line of Hilbert scanning, the method would be disabled. Also this method assumes that only pixel locations change do not their intensities, but the MR images which are taken at different time would not always have the same intensities. Cheng proposed a deformable local image descriptor called Local-to-Global Similarity (LGS) model [28]. Unfortunately, the method only has a little improvement in recall precision when compared with SIFT, also the author did not proposed the elimination method of wrong matching points.

In this paper, the authors propose an integrated matching approach which combines TPS, SURF, Spatial Associate Correspondence information (SAC), so as to respectively obtain the global information of MR images, local neighborhood information of feature points, and spatial associate correspondence information between the points in one neighborhood. According to proposed method, the Harris edge detector and SURF detector are utilized to extract the inner and edge feature points of the initial image. Then TPS transformation model is adopted to identify the matching region of the query point, which can avoid the ambiguities that might occur when an images has multiple similar regions. To improve the correct ratio of matching we propose the SAC method which is combined with SURF descriptor to match the feature points. Finally the TPS clustering method is proposed to eliminate the mismatching of the feature points. The matching/mismatching is an iterative process, and with the iterative of the process, TPS transformation model becomes more accurate, and more correctly matched points are obtained. In our experiments, the SIFT, SURF, and the proposed method are compared, and the results showed that our method is feasible and effective.

II. Overview of Proposed Approach

Fast-Hessian has been shown to be one of the most stable feature point detectors, and to be invariant to scaling, rotating and changes in illumination [25], [26]. Unfortunately, Fast-Hessian cannot detect the edge points that are very important for measuring deformation. Thus, after extracting inner feature points, which are distributed in the inner parts of the skin, fat, muscle, or organ of the biological tissues, with Fast-Hessian, the Harris operator [30] is utilized to detect the edge points of the initial images which are distributed in the boundaries and layer separatrixes of different anatomical tissues. Afterwards, the feature points are described by the SURF descriptor.

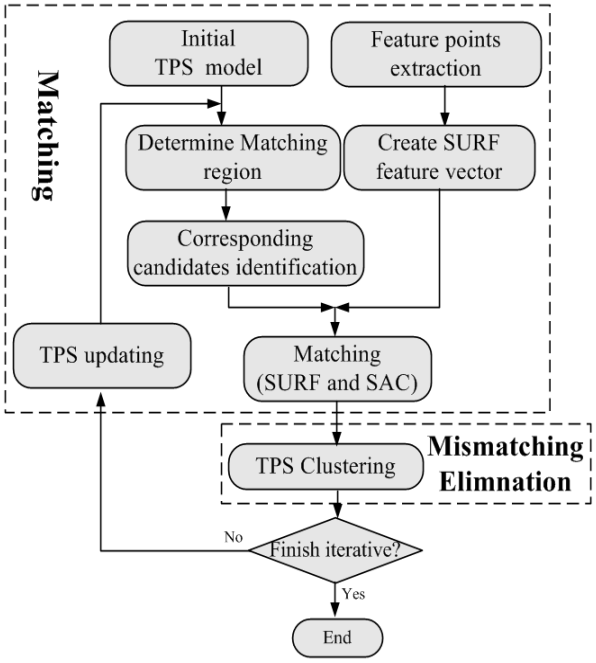

Figure. 1. The flow chart of proposed integrated method

SURF descriptor lacks global information on images, making it prone to mismatching when there are multiple similar local regions in the image. However, similar local regions usually occur in the MR images of nonrigid biological tissue. To overcome this drawback of SURF, we utilized the TPS transformation model to determine the small matching region in the deformed image for every query point in the initial image. Even in the matched region, mismatches would still occur if the feature points are matched only by the SURF descriptor. We therefore propose SAC and combine it with SURF descriptor during the matching process. The details of TPS-SURF-SAC matching are described in Section 3.

After TPS-SURF-SAC matching of the feature points, the TPS clustering method is adopted to eliminate the residual mismatching points. We introduce a difference vector, consisting of the coordinate differences between the points matched by TPS and TPS-SURF-SAC. This is followed by use of the clustering method of difference vectors to identify the correctly matched points, which are determined by the maximum cluster of difference vectors. The details of the TPS clustering method is described in Section 4.

The elimination of mismatches using TPS clustering is dependent on the TPS transformation. Since the initial TPS model determined by several landmarks is not accurate, only a small number of correctly matched points could be identified after clustering based on the initial TPS model. To solve this problem, we repeat the processes of matching and elimination of mismatches, such that TPS and feature point matching reinforce each other. After every iterative matching and

elimination of mismatching, we obtain more correctly matched points to improve the TPS model, making it closer to the real deformation of tissues. In addition, the matched regions determined by TPS model would be more accurate, and the results of mismatching elimination by TPS clustering should also be improved, until the processing is stable.

III. MATCHING

A. *Identification of the matching region - TPS*

Thin Plate Spline is an interpolation method that finds a "minimally bended" smooth surface that passes through all given points [31], [32]. It is particularly popular in representing shape transformations, such as image morphing or shape detection and matching. TPS maps any location $\mathbf{x} = [x, y]^T$ to a new location $\mathbf{x}' = [x', y']^T$ as follows:

$$\mathbf{x}' = T_{tps}(\mathbf{x}) = A(\mathbf{x}) + R(\mathbf{x}), \quad (1)$$

where A(**x**) denotes the global affine transformation and R(**x**) represents the non-global (non-linear) transformation, with the latter described by a radial basis function. Given a set of control points, TPS transformation can map any location x to a new location **x**'.

TPS can accurately measure non-linear deformation between images if there are enough correctly matched and well distributed control points. If there are only a few control points distributed globally throughout the images, an approximate deformable transformation of the deformed image can be obtained. Based on the TPS transformation, we can identify a small local region around the TPS mapping point corresponding to the query point, and the real point corresponding to the query point could be located in the local region with high probability. The local region is named "Matching Region". The initial TPS model are determined by several landmark points distributed somewhat uniformly in the initial and deformed MR images, and the matching region of query points are identified based on the initial TPS model.

B. *SURF descriptor*

The SURF descriptor describes how the pixel intensities are distributed within a scale dependent neighborhood of each interest point detected by the Fast-Hessian [25], [26].

1) Orientation Assignment: To determine the orientation, Haar wavelet responses of size 4σ are calculated for a set of pixels around the detected point with a radius of 6σ, where σ refers to the scale at which the point was detected.

Once the wavelet responses are weighted with a Gaussian (2.5σ) centered at the interest point, they are represented as vectors in space with the horizontal response strength along the abscissa and the vertical response strength along the ordinate. The dominant orientation is estimated by calculating the sum of all responses within a sliding orientation window covering an angle of π/3. The longest responses vector lends its orientation to the interest point.

2) Descriptor Components: The first step in extracting the SURF descriptor is to construct a square window around the interest point. This window contains the pixels which will form entries in the descriptor vector and is of size 20σ. Furthermore, the window is oriented along the dominant orientation such that all subsequent calculations are relative to this direction.

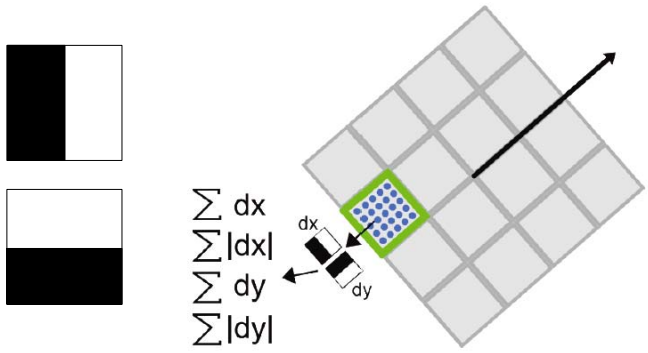

Figure. 2. Left: Haar wavelet types for SURF (top the x-direction and bottom the y-direction). Right: SURF descriptor component. The brown arrow directs the dominant orientation, and the green rectangle refers to one of the descriptor subregion.

As shown in Fig. 2 the descriptor window is divided into 4 ×4 regular subregions. Within each subregion Haar wavelets of size 2σ are calculated for 25 regularly distributed sample points. Letting dx and dy be wavelet responses along x- and y-axes, respectively, we collect dx, dy, |dx|, and |dy| for these 25 sample points (i.e. each subregion),

$$v_{subregion} = \left[\sum dx, \sum dy, \sum |dx|, \sum |dy|\right]. \quad (2)$$

Therefore each subregion contributes four values to the descriptor vector leading to an overall vector of length 64.

C. *Spatial association correspondence-SAC*

1) Corresponding candidates: Although the target points are within the small matching region calculated by TPS model, the SURF matching point with minimum SURF descriptor distance from the query point may not always be corresponding point. In this paper, we introduce a threshold t_{SURF} for any query point P, such that t_{SURF} should be larger than the SURF distance between P and its corresponding point. The target point whose SURF distance from P is less than t_{SURF} is defined as a corresponding candidate of P. Every query point has a certain number of corresponding candidates (the green points) in its matching region. As t_{SURF} decreases, so would the number of corresponding candidates. However, if t_{SURF} is too small, the real corresponding point may be excluded from the set of corresponding candidates. The purpose of SAC is to identify the corresponding point from among the candidates.

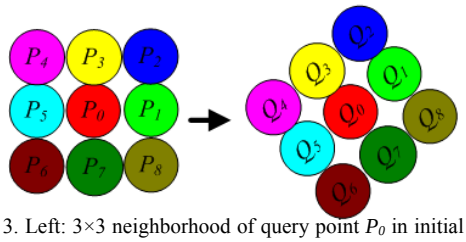

Figure. 3. Left: 3×3 neighborhood of query point P_0 in initial image. Right: 3×3 neighborhood of corresponding point Q_0 in deformed image.

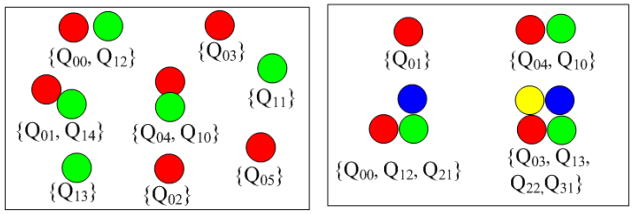

(a) (b)

Figure. 4. Corresponding probability comparison of the corresponding candidates.

2) Spatial association correspondence supposition: Although non rigid tissues are deformed in MR images, in very small regions, such those measuring 3×3 pixels, it is likely that pixels neighboring the region of the initial image would also be neighboring the corresponding region of the deformed image. Usually the feature points extracted by Fast-Hessian and Harris would be more stable to deformation than that of the general points of the images. Actually, although not all the feature points would obey SAC supposition, it would be useful for point matching as long as a considerable number of stable feature points can satisfy the SAC supposition. The neighborhood of query point P_0 in the initial image and the neighborhood of target point Q_0 in the deformed image are shown in Fig. 3. The circles of different colors refer to pixel points of the neighborhood located in different positions. Based on the SAC, if query point P_0 corresponds to the target point Q_0, P_1 would probably correspond to Q_1, and points P_2 through P_8 would probably correspond to Q_2 though Q_8, respectively.

3)Probability of Corresponding: Several terms:

a) $S_j = (Q_{j0}, Q_{j1}, \ldots, Q_{jk_j})$: the set of candidates corresponding to P_j (j=0, 1, 2, … , 8).

b) $Pr(Q_{ji})$: Probability that Q_{ji} corresponds to P_j.

c) $SAC\ (Q_{0k_0}, Q_{1k_1}, \ldots, Q_{jk_j})$: the discriminant of SAC.

If the relative positions without considering the rotation of Q_{0k_0} through Q_{jk_j} coincide with those of P_0 through P_j, then the discriminant $SAC(Q_{0k_0}, Q_{1k_1}, \ldots, Q_{jk_j}) = True$, otherwise the SAC discriminant is equal to *False.*

d) $N_{SAC}(Q_{0k_0}, Q_{1k_1}, \ldots, Q_{jk_j})$: the number of points that obey the SAC supposition in the neighborhood of feature point.

TABLE 1
SAC ALGORITHM

SAC algorithm

1) Initialize a chain set C.

Ⅰ. Input all the points of S_0 (S_0 is the set of corresponding candidates of P_i) into set C.

2) Search all the points of S_1.

Ⅰ. IF $\{Q_{0k_0}\} \in C$, $Q_{1k_1} \in S_1$; and $SAC\ (Q_{0k_0}, Q_{1k_1}) = True$, THEN create a new element $\{Q_{0k_0}, Q_{1k_1}\}$ and input it into C;

Ⅱ. Delete the elements which consist of only one point.

3) Search all the points of S_2.

Ⅰ. IF $\{Q_{0k_0}, Q_{1k_1}\} \in C$, $Q_{2k_2} \in S_2$; and $SAC(Q_{0k_0}, Q_{1k_1}, Q_{2k_2}) = True$, THEN create new element $\{Q_{0k_0}, Q_{1k_1}, Q_{2k_2}\}$ and input into C;

Ⅱ. Delete the elements which consist of only two points.

4) Search all the points of S_i, ($3 \leqslant i \leqslant 8$).

Ⅰ. Repeat the same process as step 2) and 3);

Ⅱ. IF only one element $\{Q_{0k_0}, Q_{1k_1}, \ldots\} \in C$, THEN Q_{0k_0} is the corresponding point of P_0;

Ⅲ. Else IF $C = \phi$, back up to the results of previous step, THEN go to 5);

Ⅳ. Or else IF after S_8 is processed, still more than one element is left in C, THEN go to 5).

5) Compare the SURF distance.

For the first point of every element in C, compare their SURF distances to P_0. The candidate of the least SURF distance is corresponding point of P_0.

If the SAC discriminant of Q_{0k_0} through Q_{jk_j} is equal to *True*, then $N_{SAC}(Q_{0k_0}, Q_{1k_1}, \ldots, Q_{jk_j})$ is equal to j; otherwise it is equal to $N_{SAC}(Q_{0k_0}, Q_{1k_1}, \ldots, Q_{j-1,k_{j-1}})$.

According to SAC supposition, if P_0 corresponds to Q_0, the neighboring points P_1 though P_8 would likely correspond to Q_1 though Q_8. Conversely, if a target point Q_{0k_0} is a corresponding candidate of P_0, and the neighboring points of Q_{0k_0} are the corresponding candidates of P_1 to P_8, respectively, that is, the SAC discriminant of Q_{0k_0} through Q_{jk_8} is equal to *True*, then Q_{0k_0} has high probability of $Pr(Q_{0k_0})$ corresponding to P_0. Based on this inference, two *Comparison Rules* of corresponding probability can be formulated. Suppose Q_{0k_0} and Q'_{0k_0} are two corresponding candidates of P_0. Then,

a) If

$N_{SAC}(Q_{0k_0}, Q_{1k_1}, \ldots, Q_{jk_j}) > N_{SAC}(Q'_{0k_0}, Q'_{1k_1}, \ldots, Q'_{jk_j})$

then $Pr(Q_{0k_0}) > Pr(Q'_{0k_0})$.

b) If

$N_{SAC}(Q_{0k_0}, Q_{1k_1}, \ldots, Q_{jk_j}) = N_{SAC}(Q'_{0k_0}, Q'_{1k_1}, \ldots, Q'_{jk_j})$

then, if $DIS(P_0, Q_{0k_0}) < DIS(P_0, Q'_{0k_0})$ then $Pr(Q_{0k_0}) > Pr(Q'_{0k_0})$, and vise versa, where $DIS(P_j, Q_{jk_j})$ denotes the SURF distance between P_j and Q_{jk_j}.

According to the above *Comparison Rules*, the comparison results of corresponding probabilities in Fig. 4-(a) and (b) are shown as:

$$\Pr(Q_{0i}) > \Pr(Q_{0j}) \quad (i = 0, 1, 4; j = 2, 3, 5), \tag{3}$$

$$\Pr(Q_{03}) > \Pr(Q_{00}) > \Pr(Q_{04}) > \Pr(Q_{01}) . \tag{4}$$

4) Identification of corresponding point-SAC algorithm: Based on the supposition of SAC and the probability analysis of the candidates corresponding to the query point, we proposed the SAC algorithm to identify the corresponding point of any query point P_0 as Table 1.

IV. Mismatching Elimination

A. Definition of difference clustering

Recall that **x** and **x'** are the coordinate vectors of a query point P and its matching point P' obtained by TPS transformation. Let P'' be the matching point of P obtained by the TPS-SURF-SAC matching method, and $\mathbf{x}'' = [x'', y'']^T$ be the coordinate vector of P'', and $\mathbf{d} = [d^x, d^y]^T$ be the difference coordinate vector:

$$\mathbf{d} = \mathbf{x}'' - \mathbf{x}' . \tag{5}$$

Clustering is a method of unsupervised learning. In this paper, every difference coordinate vector can be taken as the clustering center. Let $\mathbf{d}_i = [d_i^x, d_i^y]^T$ be the cluster center and $\mathbf{d}_j = [d_j^x, d_j^y]^T$ be any difference coordinate vector. Let Clt_i be the i-th cluster with its center $\mathbf{d}_i$ and radius R. If

$$dist(\mathbf{d}_i - \mathbf{d}_j) \le R , \tag{6}$$

where *dist* is the distance of infinite norm, then

$$\mathbf{d}_j \in Clt_i . \tag{7}$$

We take every difference coordinate vector as the clustering center, and the matching points corresponding to the difference coordinate vectors in the maximum cluster are considered the correctly matched points.

B. Update of the TPS model

Because the initial TPS model was calculated using several landmark points, it is not accurate for real deformation. So, by means of the clustering based on the initial TPS model, most of the correctly matched points far from the landmarks cannot be identified. The accuracy of the TPS model is decided by the correctly matched points, with more correctly matched points resulting in a more accurate TPS model. After TPS clustering, we can obtain a certain number of correctly matched points, which are used in turn to update the TPS model. Afterward, the matching and mismatching processes are repeated based on the new TPS model. Matching and elimination of mismatching are performed iteratively. With each iteration, more correctly matched points can be identified after TPS clustering and the TPS model can be updated to more accurately reflect the real deformation of the tissues.

V. Experiment Results

In our experiments, SIFT, SURF, and the proposed integrated method are compared. The initial and deformed MR images of volunteer's abdomen are tested. The images are taken by the 0.5T open MRI device, of which the FOV is 24×24cm^2. The tow sets of images show deformations of the abdomen when pushing and pressing on the kyte, named AbdPush and AbdPress respectively. For the SIFT and SURF methods, the image pyramids each consisted of 3 octaves, with every octave having 4 levels with different scales. After the feature points were extracted, the NN/SCN (the ratio of the nearest and second nearest neighbors) of SURF distance was adopted to match the feature points of the initial and the deformed MR images.

The experimental results of SIFT are shown in Fig. 5. Only 23 and 65 pairs of points are matched in AbdPush and AbdPress, respectively. The numbers of outliers are 4 and 5 in the matching pairs of AbdPush and AbdPress, respectively. As similar with the experimental results of SIFT, 20 and 32 pairs of points are matched by SURF, and 3 and 6 pair of points are wrong matched in AbdPush and AbdPress, respectively (Fig. 6). Although the correctly matched ratios of SIFT are 82.61% and 91.8%, and the correctly matched ratios of SURF are 85.0% and 81.25%, respectively, the correctly matched points are too few to obtain the accurate physical characteristics distributed all over the nonlinear tissues.

The experiment results of proposed method are shown in Fig. 8. From the results we can see that a number of points are matched by TPS-SURF-SAC. In AbdPush and AbdPress, 174 and 180 pairs of points are matched, with the numbers of wrong matching pairs only being 2 and 1, respectively. The correctly matched ratios are higher than that of SIFT and SURF. Especially, in the parts of large deformation, many matching points are still obtained by TPS-SUR-SAC, which is significant for deformation measurement.

To prove the effectiveness of the proposed SAC method, we have tested our method without SAC during the matching processing, for briefly, being referred to as TPS-SURF. The experimental results are shown in Fig. 7. We find that 138 and 178 pairs of feature points are matched, and 12 and 5 pairs of

feature points are wrong matched in AbdPush and AbdPress, respectively. The correctly matched ratios are both lower than that of TPS-SUR-SAC. Table 2 shows the comparison of the experimental results by SIFT, SURF, TPS-SURF and TPS-SURF-SAC. From this table, we can see that the proposed integrated method can obtain much more correctly matched points, and eliminate most of the wrong matched points as well. The SAC is useful to the matching of the feature points from the blurred and obscure MR images.

TABLE 2

Comparison of Experimental Results of Four Methods

MR image	Method	NM	NCM	NWM	Ratio(%)
AbdPush	SIFT	23	19	4	82.61
	SURF	20	17	3	85.0
	TPS-SURF	138	126	12	91.3
	TPS-SURF-SAC	174	172	2	98.85
AbdPress	SIFT	61	56	5	91.8
	SURF	32	26	6	81.25
	TPS-SURF	178	173	5	97.19
	TPS-SURF-SAC	180	179	1	99.44

NM: Number of the matched pairs; NCM: Number of correctly matched pairs; NWM: Number of incorrectly matched pairs; Ratio: correctly matched ratio.

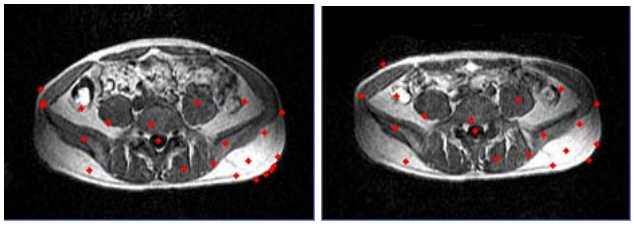

(a) The results of AbdPush

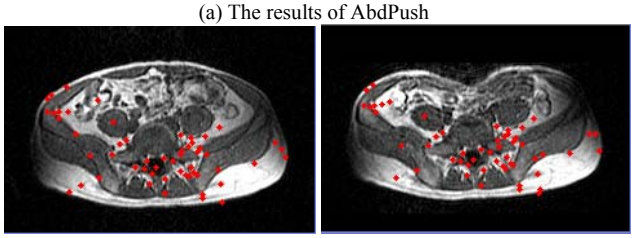

(b) The results of AbdPress

Figure 5. The experimental results by SIFT.

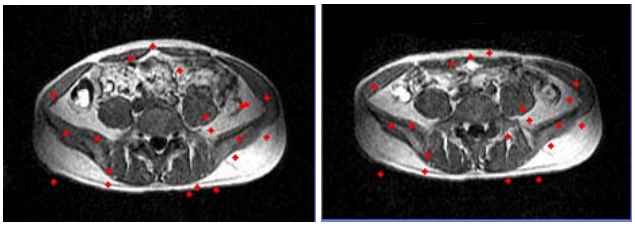

(a) The results of AbdPush

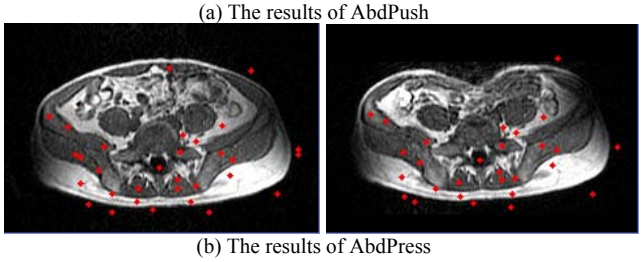

(b) The results of AbdPress

Figure 6. The experimental results by SURF.

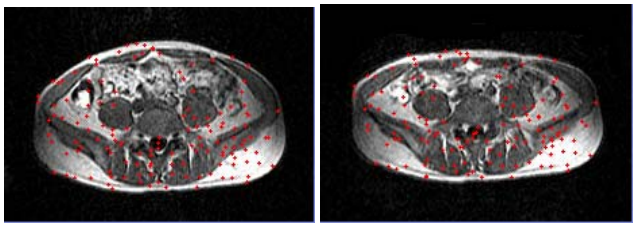

(a) The results of AbdPush

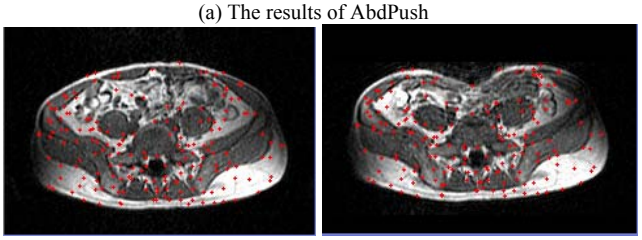

(b) The results of AbdPress

Figure 7. The experimental results by TPS-SURF.

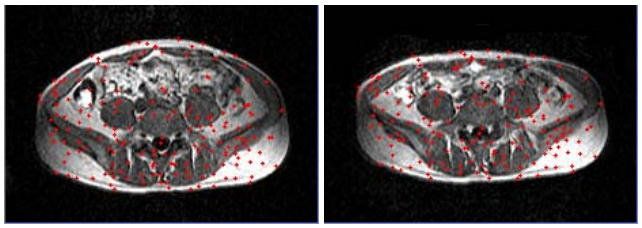

(a) The results of AbdPush

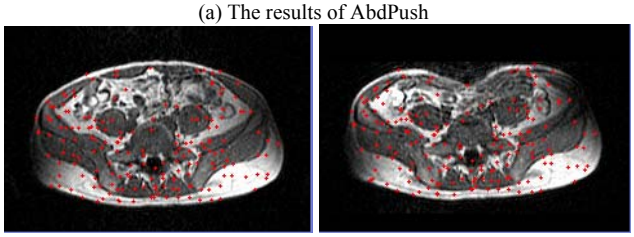

(b) The results of AbdPress

Figure 8. The experimental results by TPS-SURF-SAC.

VI. Conclusion

The matching of feature points are important in many research and application fields, while in this paper we focus on the deformation measurement of nonrigid, nonuniform biological tissues from MR images which are usually blurred, obscure and with low resolutions.

In this paper, SURF and Harris operator are utilized to extract the inner and edge feature points respectively. During the matching process, the matching region of the query point is determined by TPS transformation model. Then the proposed SAC method is combined with the SURF descriptor to identify the corresponding point. To eliminate the mismatching of the feature points, TPS clustering method is utilized to identify the correctly matched points. The matching and mismatching elimination process is iterative, with the iterative of the process, more correctly matched points are obtained, and the TPS model becomes closer to the real deformation, until the number of the correctly matched points becomes stable.

In the experiments, SIFT, SURF, and proposed integrated method are compared in the feature points matching of the MR images of the volunteer's abdomen. The experiment

results show that the proposed integrated method could detect much more correctly matched points, and the correctly matched ratio is much higher as well, those are very important to the accurate measurement of deformation field.

We can draw the following conclusions. Firstly SAC is valid to the feature point matching of deformed tissues from MR image. Secondly, TPS clustering can eliminate most incorrectly matched pairs, and the correctly matched point and the TPS model can be boosted by each other.

The proposed method also has some limitations, such as a higher computation cost than SIFT and SURF, and we have to choose some landmarks for calculation of the initial TPS model between the initial and deformed images.

ACKNOWLEDGMENT

This research was supported by JSPS Grant in Aid for Scientific Research (No.2324604) and R-GIRO program of Ritsumeikan University, Japan. This work is partially supported by Prof. Shigerhiro Morikawa in Shiga University of Medical Science, Japan. The authors also gratefully acknowledge the helpful suggestions of Prof. Penling Zhang in Wuhan University, China.

REFERENCES

[1] P. L. Zhang, S. Hirai, K. Endo, and S. Morikawa, "Local deformation measurement of biological tissues based on feature tracking of 3D MR volumetric images," in *Proc. 2007 IEEE/ICME Int. Conf. Complex Medical Engineering*, 2007, pp. 707-711.

[2] P. L. Zhang, S. Hirai, and K. Endo, "A feature matching-based approach to deformation fields measurement from MR images of non-rigid object," *International Journal of Innovative Computing, Information and Control*, vol.4, pp. 1607–1625, 2008.

[3] P. L. Zhang and S. Hirai, "A local geometric preserving approach for interior deformation fields measurement from MR volumetric images of Human Tissues," in *Proc. Proceedings of 2010 IEEE International Conference on Robotics and Biomimetics*, Tianjin, China, 2010, pp. 437-441.

[4] Z. K. Wang, K. Namima, and S. Hirai, "Physical parameter identification of uniform rheological deformation based on FE simulation," *Trans. Japanese Society for Medical and Biological Engineering*, vol. 47(1), pp. 1-6, Feb. 2009.

[5] Z. K. Wang, K. Namima, and S. Hirai, "Physical parameter identification of rheological object based on measurement of deformation and force," in *Proc. 2009 IEEE Int. Conf. Robotics and Automation (ICRA 2009)*, Kobe, May. 2009, pp. 1047-1052.

[6] D. Rueckert, L. I. Sonoda, C. Hayes, D.L.G. Hill, M.O. Leach, and D.J. Hawkes, "Non-rigid registration using free-form deformations: Application to breast MR images," *IEEE Transactions on Medical Imaging*, vol. 18(8), pp. 712-721, 1999.

[7] T. Rohlfing, Jr. CR. Maurer, D.A. Bluemke, and M.A. Jacobs, "Volume-preserving nonrigid registration of MR breast images using free-form deformation with an incompressibility constraint," *IEEE Transactions on Medical Imaging*, vol. 22(6), pp. 730-741, 2003.

[8] Z. Xie, G.E. Farin, "Image registration using hierarchical B-splines," *IEEE Transactions on Visualization and Computer Graphics*, vol. 10(1), pp. 85-94, 2004.

[9] N.J. Tustison, B.A. Avants, and J.C. Gee, "Improved FFD B-Spline image registration", in *Proc. IEEE 11th International Conference on Computer Vision (ICCV 2007)*, Rio de Janeiro, Brazil, 2007, pp. 1-8.

[10] J.P. Thirion, "Image matching as a diffusion process: an analogy with maxwell's demons," *Medical Image Analysis*, vol. 2(3), pp. 243–260, 1998.

[11] T. Vercauteren, X. Pennec, A. Perchant and N. Ayache, "Non-parametric diffeomorphic image registration with the Demons algorithm," in *Proc. Proceedings of the 10th International Conference on Medical Image Computing and Computer Assisted Intervention (MICCAI 2007)*, Brisbane, Australia, 2007, vol. 4792, pp. 319-326.

[12] N. D. Cahill, J. A. Noble1, and D. J. Hawkes, "A Demons algorithm for image registration with locally adaptive regularization," in *Proc. Proceedings of the 12th International Conference on Medical Image Computing and Computer Assisted Intervention (MICCAI 2009)*, 2009, vol.12, pp. 574-581.

[13] M. F. Beg, M. I. Miller, A. Trouvé, and L. Younes, "Computing large deformation metric mappings via geodesic flows of diffeomorphisms," *International Journal of Computer Vision*, vol. 61(2), pp.139-157, 2005.

[14] T. Vercauteren, X. Pennec, Aymeric Perchant, and N. Ayache, "Diffeomorphic Demons: Efficient Non-parametric Image Registration," *NeuroImage*, vol. 45(1), pp. s61-s72, 2009.

[15] D. Shen, and C. Davatzikos, "HAMMER: hierarchical attribute matching mechanism for elastic registration," *IEEE Transactions on Medical Imaging*, vol. 21(11), pp. 1421-1439, 2002.

[16] G. Wu, Q. Wang, H. Jia, and D. Shen, "Feature-based groupwise registration by hierarchical anatomical correspondence detection," in *Proc. Proceedings of the 13th International Conference on Medical Image Computing and Computer Assisted Intervention (MICCAI 2010)*, Beijing, China, 2010, vol.13(2), pp. 684-691.

[17] L. Shu, A.C.S. Chung, "Feature based nonrigid brain MR image registration with symmetric alpha stable filters," *IEEE Transactions on Medical Imaging*, vol. 29(1), pp.106-119, 2010.

[18] G. Wu, F. Qi, and D. Shen, "Learning best features and deformation statistics for hierarchical registration of MR brain images", in *Proc. Information Processing in Medical Imaging, 20th International Conference (IPMI 2007)*, Kerkrade, The Netherlands, 2007, vol. 4584, pp. 160-171.

[19] T. Lange, N. Papenberg, S. Heldmann, J. Modersitzki, B. Fischer, and H. Lamecker et al., "3D ultrasound-CT registration of the liver using combined landmark-intensity information," *International Journal of Computer Assisted Radiology and Surgery*, vol. 4(1), pp. 79-88, 2008.

[20] D. G. Lowe, "Distinctive image features from scale-invariant keypoints," *International Journal of Computer Vision*, vol. 60, pp. 91–110, 2004.

[21] Y. Ke, and R. Sukthankar, "PCA-SIFT: A more distinctive representation for local image descriptors," *Computer Vision and Pattern Recognition*, vol. 2, pp. 506–513, 2004.

[22] K. Mikolajczyk, and C. Schmid, "A performance evaluation of local descriptors," *IEEE Transactions on Pattern Analysis and Machine Intelligence*, vol. 27, pp.1615–1630, 2005.

[23] L. M. J. Florack, B. M. Ter Haar Romeny, J. J. Koenderink, and M. A. Viergever, "General intensity transformations and differential invariants," *Journal of Mathematical Imaging and Vision*, vol. 4, pp. 171–187, 1994.

[24] F. Mindru, T. Tuytelaars, L. van Gool, and T. Moons, "Moment invariants for recognition under changing viewpoint and illumination," *Computer Vision and Image Understanding*, vol. 94, pp. 3–27, 2004.

[25] H. Bay, T. Tuytelaars, and L. V. Gool, "SURF：Speeded Up Robust Features," in *Proc. 9th European Conference on Computer Vision (ECCV 2006)*, Graz, Austria, 2006, pp.404 -417.

[26] H. Bay, A. Ess, T. Tuytelaars, and L. V. Gool, "Speeded-up Robust Features (SURF)," *Computer Vision and Image Understanding*, vol. 110, pp. 346-359, March, 2008.

[27] H. Lin and D. W. Jacobs, "Deformation invariant image matching," In *Proc. 10th IEEE International Conference on Computer Vision (ICCV, 2005)*, pp.1466–1473, 2005.

[28] H. Cheng, Z. C. Liu, N. Zheng and J. Yang, "A deformable local image descriptor," In *Proc*, *IEEE Conference on Computer Vision and Pattern Recognition (CVPR 2008)*, 2008, pp. 1-8.

[29] L. Tian and S. I. Kamata. A Low-Complexity Deformation Invariant Descriptor. In *Proc*, *18th International Conference on Pattern Recognition (ICPR 2006)*, 2006, pp. 227-230.

[30] C. Harris, and M. Stephens, "A combined corner and edge detector," In *Proc. Proceedings of the Alvey Vision Conference*, 1988, pp.147-151.

[31] F. L. Bookstein, "Principal warps: Thin-Plate Splines and the decomposition of deformations," *IEEE Transactions on Pattern Analysis and Machine Intelligence*, vol. 11(6), pp. 567-585, 1989.

[32] B. Zitová and J. Flusser, "Image registration methods: a survey," *Image and Vision Computing*, vol. 21(11), pp. 977-1000, 2003.